Computer Assisted Mechanics and Engineering Sciences, 13: 473–480, 2006.

Structural inverse problems solved by the T-element approach

Adam Wróblewski, Andrzej P. Zieliński
Cracow University of Technology, al. Jana Pawła II 37, Kraków, Poland

(Received March 17, 2006)

Any direct boundary-value problem is defined in a certain area Ω by a system of differential equations and respective set of boundary conditions. In structural inverse problems the above conditions can be partly unknown. Instead, we can measure certain quantities inside the investigated structure and then approximately define the whole boundary-value problem. Usually, the solutions of inverse problems are connected with the minimization of a certain functionals, which results in optimization procedures. The applications of the trial functions identically fulfilling governing partial differential equations of a discussed problem (the Trefftz approach) can considerably improve these procedures.

The original idea of Erich Trefftz was based on modelling objects of simple geometry. In the case of more complex structures the division of the whole object into sub-regions (Trefftz elements) is necessary. This kind of formulation is presented in this paper and is illustrated by numerical examples. The properties of the Trefftz finite elements allow the formulation of effective algorithms, which considerably shorten the time of computer calculations in comparison to standard finite element solutions.

1. Introduction

The family of contemporary Trefftz-type methods of modelling, in which trial functions (T-functions) identically fulfil governing differential equations of a boundary-value problem, can be divided into two main groups, i.e. global-type formulations and sub-structuring methods. In the first group the trial functions are defined in a whole investigated domain Ω, while in the second formulation their sets are formed in many sub-areas Ω_e with boundaries Γ_e.

In the previous paper concerning the application of the Trefftz approach to inverse problems of elasticity [5], the global version of the method was investigated. Three different concepts of inverse problem solutions have been proposed showing a good convergence of results and encouraging the authors to undertake further research. However, the shapes of considered areas Ω were rather simple. If a form of an investigated structure is more complex, this global approach cannot be applied because difficulties with conditioning of the final algebraic equations can appear. Therefore, we are forced to introduce sub-structuring, for example in the form of the Trefftz finite elements (T-elements) [3, 4, 6]. Application of such elements to inverse problems in 2D elasticity is a topic of the present work.

The most popular T-elements follow the J. Jirousek's ideas [1, 2]. In the HT-D formulation the element stiffness matrix (2D elasticity) has a symmetric and positive definite form

$$\mathbf{k} = \mathbf{G}^{-1}\mathbf{H}\mathbf{G} \tag{1}$$

where

$$\mathbf{G} = \int_{\Gamma^e} \mathbf{T}^{\mathrm{T}}\tilde{\mathbf{N}}\,\mathrm{d}\Gamma, \tag{2}$$

$$\mathbf{H} = \int_{\Gamma^e} \mathbf{T}^{\mathrm{T}}\mathbf{N}\,\mathrm{d}\Gamma = \int_{\Gamma^e} \mathbf{N}^{\mathrm{T}}\mathbf{T}\,\mathrm{d}\Gamma. \tag{3}$$

The matrices $\mathbf{N}$ and $\mathbf{T}$ appear in displacements

$$\mathbf{u}(\mathbf{x}) = \mathring{\mathbf{u}}(\mathbf{x}) + \mathbf{N}(\mathbf{x})\,\mathbf{c} \qquad \mathbf{x} \in \Omega_e\,, \tag{4}$$

$$\tilde{\mathbf{u}}(\mathbf{x}) = \tilde{\mathbf{N}}(\mathbf{x})\,\mathbf{d} \qquad \mathbf{x} \in \Gamma_e\,, \tag{5}$$

and tractions

$$\mathbf{t}(\mathbf{x}) = \mathring{\mathbf{t}}(\mathbf{x}) + \mathbf{T}(\mathbf{x})\,\mathbf{c} \qquad \mathbf{x} \in \Gamma_e\,, \tag{6}$$

where $\mathbf{N}$ is a matrix of the Trefftz functions, $\tilde{\mathbf{N}}$ is a matrix of polynomials defined along the boundary Γ_e, $\mathbf{T}$ represents respective tractions, $\mathbf{c}$, $\mathbf{d}$ are unknown coefficients and $\mathring{\mathbf{u}}$, $\mathring{\mathbf{t}}$ are particular solution parts of the displacements and tractions, respectively. The details of the element formulation can be found, for example, in [2]. This element implemented into the FE system SAFE [1] has been used in this particular study.

In the HT-D element number of the inside Trefftz functions in $\mathbf{N}$ is strictly connected with the number of the polynomial functions in $\tilde{\mathbf{N}}$ (see [3]). In the present investigations the authors used quadrilateral elements and the number of T-functions was always equal $N_{\mathrm{T}} = 4p$ (p – degree of polynomials) for each of the two displacements in $\mathbf{u}$.

2. General formulation of discussed inverse problems

Let us consider a 2D elastic plate loaded in a self-equilibrated way (Fig. 1). The load $\bar{q}(x)$ in its upper part is unknown. Instead, we can measure stresses in a certain number of control points placed in a distance δ from the "hidden" edge. In general, the measurement points can be situated in different places, however, in this paper we restrict their positions to a straight line. The aim of the calculations is a possibly accurate definition of the full, original boundary-value problem of the investigated object.

If the unknown load is assumed to be linear along external boundaries of the particular finite elements, then it can be defined by its values q_k in the element corners along the object boundary.

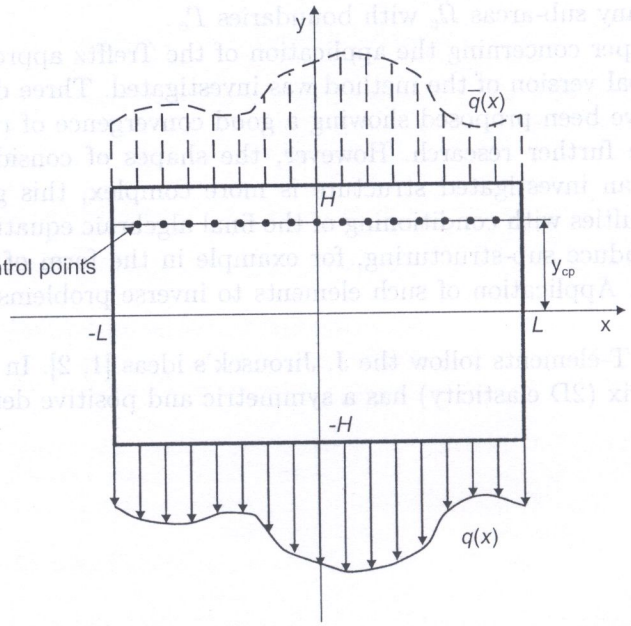

Fig. 1. Elastic plate; $\bar{q}(x)$ are unknown boundary tractions

Hence, the solution means minimization of the following functional with respect to the unknown coefficients q_k,

$$\Phi = \sum_{i=1}^{N} \left[(\sigma_x - \bar{\sigma}_x)^2 + (\sigma_y - \bar{\sigma}_y)^2 + (\sigma_{xy} - \bar{\sigma}_{xy})^2 \right] \to \min_{q_k}, \tag{7}$$

where $\bar{\sigma}_{ij}$ are known, measured values of stresses in the N control points. Additionally, the searched load function should fulfill a global equilibrium condition. In the case of a vertical load (Fig. 1) it can in general be written as

$$\int_{-L}^{L} [q(x) + \bar{q}(x)] \, \mathrm{d}x = 0, \tag{8}$$

$$\int_{-L}^{L} x \, [q(x) + \bar{q}(x)] \, \mathrm{d}x = 0. \tag{9}$$

The investigations of the present paper are focused on effectiveness of the Trefftz finite element approach. Therefore, in the optimization procedures the authors applied standard gradient methods. The proposed algorithms are presented below in a series of numerical examples.

3. Numerical investigations

To investigate the inverse problems, the quadratic plate ($L = H = 1.0$) compressed along two opposite sides by vertical tractions

$$q(x) = 100(1 - x^2), \tag{10}$$

$$\bar{q}(x) = -100(1 - x^2), \tag{11}$$

was chosen as the first numerical example. Because of the symmetry condition with respect to the axis y, only half of the plate was considered (symmetry with respect to x was not known *a priori*).

In this case the additional equilibrium equation can be written as

$$\int_0^L q(x) \, \mathrm{d}x = \sum_{k=2}^{K} \frac{q_k - q_{k-1}}{2} (x_k - x_{k-1}) = \int_0^L 100 \left(1 - x^2\right) \mathrm{d}x = \frac{200}{3} L. \tag{12}$$

Table 1 presents a comparison of results obtained with the help of the hybrid Trefftz elements (HT) and the conventional hierarchic p-elements (CH). The decrease of values of the objective function in case of the T-elements is distinctly visible. The most characteristic results are also presented in Fig. 2.

Table 1. Objective function (7) in example 1; HT – Trefftz elements, CH – conventional hierarchic p-elements, p – polynomial degree, $y_{\mathrm{cp}} = 0.8$, $N = 21$ control points

Mesh	Elements	$p = 2$	$p = 3$	$p = 4$	$p = 5$
2×2	HT	21.9650	17.9381	11.0777	10.7043
	CH	100.178	21.1059	201.806	205.458
4×4	HT	1.72964	0.20694	0.04121	0.01733
	CH	4.03380	0.56192	5.79732	5.52918
8×8	HT	0.04917	0.00012	4.11e−6	4.28e−6
	CH	0.51566	0.00764	0.00453	0.00450
16×16	HT	0.00899	2.15e−6	3.73e−7	3.67e−7
	CH	0.03744	0.00952	0.00962	0.00962

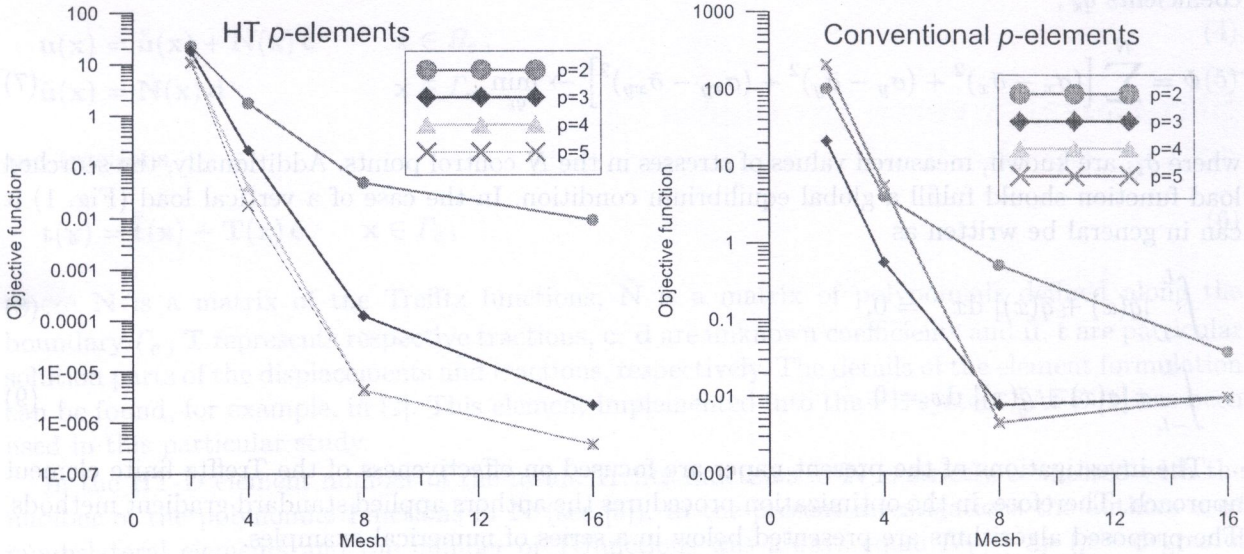

Fig. 2. Objective function (7) in example 1; $y_{\mathrm{cp}} = 0.8$, $N = 21$

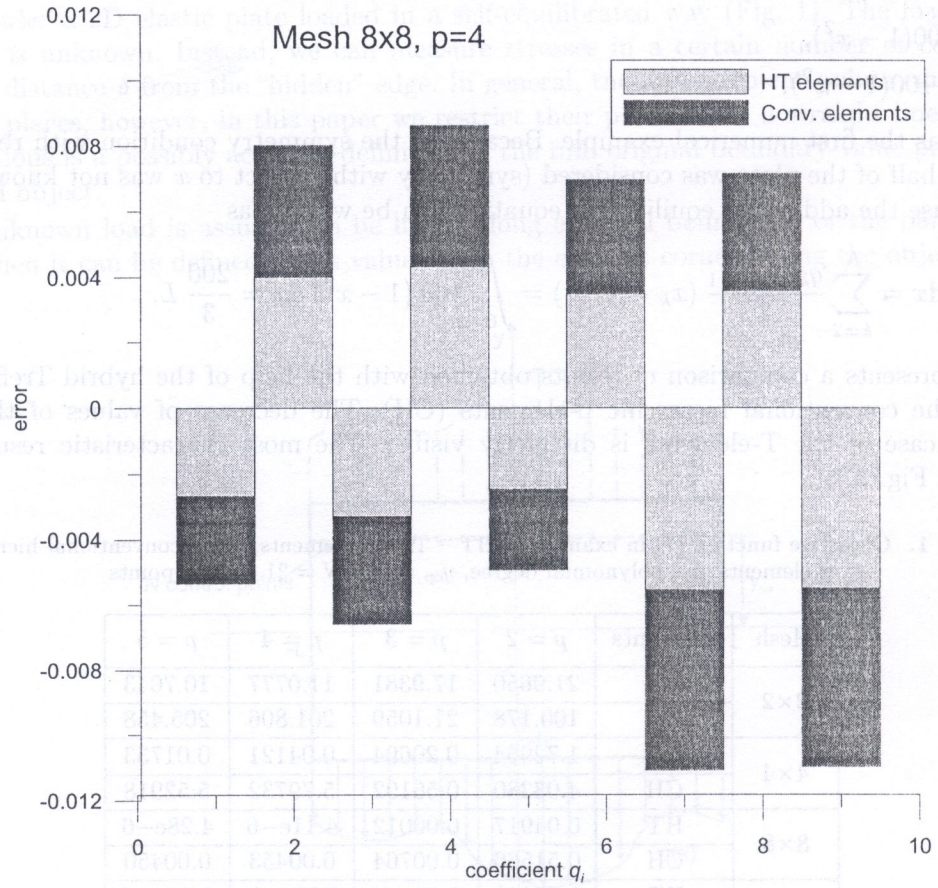

Fig. 3. Example 1: error in coefficients q_i ; $y_{\mathrm{cp}} = 0.8$, $N = 21$

In Fig. 3 we can observe the error in the coefficients q_i, which define the unknown traction boundary condition. In the case of the conventional p-elements, the errors are much larger.

Table 2 presents the behaviour of the T-element solutions (mesh 2×2) while changing the distance of the control point line ($N = 21$) to the plate side with unknown tractions. The reference values of q_1 and q_2 were obtained by least square fit of the know parabola and its piece-wise linear approximation. The behaviour of the solution is not quite regular. The errors decrease up to $y_{\text{cp}} = 0.7$ and then increase (see also Fig. 4). This results suggest that the relation of number N of the control points to the number of T-elements along the "hidden" edge should be suitably chosen.

Similar investigations were carried out to observe sensitivity of the solutions to the number of control points. Table 3 presents the results. In this case the behaviour of the solutions is very stable and regular (see also Fig. 4). With a decrease in the number of control points the accuracy of the results regularly decreases.

Table 2. Example 1: Sensitivity of traction solutions q_k and objective function (7) to distance of control point line; T-elements, $p = 2$, $N = 21$ control points, mesh 2×2

	Reference	$y_{\text{cp}} = 0.9$	$y_{\text{cp}} = 0.8$	$y_{\text{cp}} = 0.7$	$y_{\text{cp}} = 0.5$
q_1	104.167	103.642	103.821	103.984	104.776
		0.503%	0.332%	0.176%	−0.584%
q_2	79.1667	79.6856	79.5212	79.3374	78.8303
		−0.655%	−0.448	−0.216%	0.425%
Φ	0	40.9004	21.9650	10.7990	64.0179

Table 3. Example 1: Sensitivity of traction solutions Q_k and objective function (7) to the number of control points; T-elements, $p = 2$, $y_{\text{cp}} = 0.8$, mesh 2×2

	Reference	$N = 21$	$N = 11$	$N = 5$	$N = 3$
q_1	104.167	103.821	103.574	103.100	102.851
		0.332%	0.569%	1.024%	1.263%
q_2	79.1667	79.5212	79.7850	82.2901	84.4288
		−0.448%	−0.781%	−1.419%	−1.594%
Φ/N	0	1.04596	1.26022	1.96436	2.75804

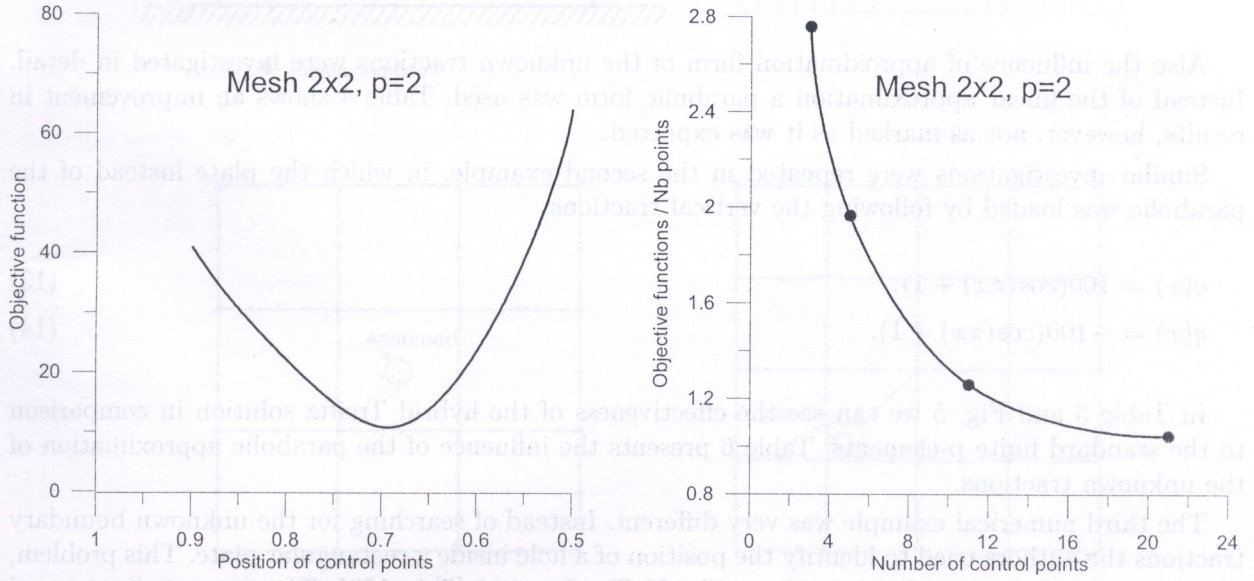

Fig. 4. Example 1: Objective function (7) vs. position y_{cp} and number N of control points

Table 4. Objective function (7) in example 1: linear vs. parabolic approximation of the boundary loads; T-element, $y_{cp} = 0.8$, $N = 21$, p – polynomial degree

Mesh	$p = 2$	$p = 3$	$p = 4$	$p = 5$
2×2 Lin	21.9650	17.9381	11.0777	10.7044
2×2 Par	3.89306	0.04723	0.01332	0.00505
4×4 Lin	1.72964	0.20694	0.04121	0.01733
4×4 Par	1.64684	0.01728	0.00277	0.00038
8×8 Lin	0.04916	0.00001	4.11e−6	4.28e−6

Table 5. Objective function (7) in example 2; HT – Trefftz elements, CH – conventional hierarchic p-elements, p – polynomial degree, $y_{cp} = 0.8$, $N = 21$

Mesh	Elements	$p = 2$	$p = 3$	$p = 4$	$p = 5$
2×2	HT	726.266	510.024	486.474	479.211
	CH	1136.00	380.432	1255.81	1233.08
4×4	HT	15.9764	1.02215	0.91026	0.53362
	CH	31.6897	13.4809	36.0473	33.3267
8×8	HT	0.58881	0.00024	5.73e−5	6.68e−5
	CH	2.86769	0.67536	0.67054	0.51835
16×16	HT	0.00658	3.41e−5	4.74e−7	5.24e−7
	CH	1.76841	1.57793	1.67970	1.18200

Table 6. Objective function (7) in example 2: linear vs. parabolic approximation of the boundary loads; T-element, $y_{cp} = 0.8$, $N = 21$

Mesh	$p = 2$	$p = 3$	$p = 4$	$p = 5$
2×2 Lin	726.267	510.025	486.474	479.211
2×2 Par	71.2762	3.47814	1.91698	1.86285
4×4 Lin	15.9764	1.02215	0.91026	0.53362
4×4 Par	14.6613	0.17263	0.00883	0.00285
8×8 Lin	0.58881	0.00025	5.73e−5	6.68e−5

Also the influence of approximation form of the unknown tractions were investigated in detail. Instead of the linear approximation a parabolic form was used. Table 4 shows an improvement in results, however, not as marked as it was expected.

Similar investigations were repeated in the second example, in which the plate instead of the parabolic was loaded by following the vertical tractions,

$$q(x) = 100(\cos(\pi x) + 1), \tag{13}$$

$$\bar{q}(x) = -100(\cos(\pi x) + 1). \tag{14}$$

In Table 5 and Fig. 5 we can see the effectiveness of the hybrid Trefftz solution in comparison to the standard finite p-elements. Table 6 presents the influence of the parabolic approximation of the unknown tractions.

The third numerical example was very different. Instead of searching for the unknown boundary tractions the authors tried to identify the position of a hole inside a rectangular plate. This problem, defined in Fig. 6a, was earlier investigated by N. Tosaka *et al.* [7] in 1995. The two coordinates and the radius of the hole made three identification variables. The boundary conditions were known

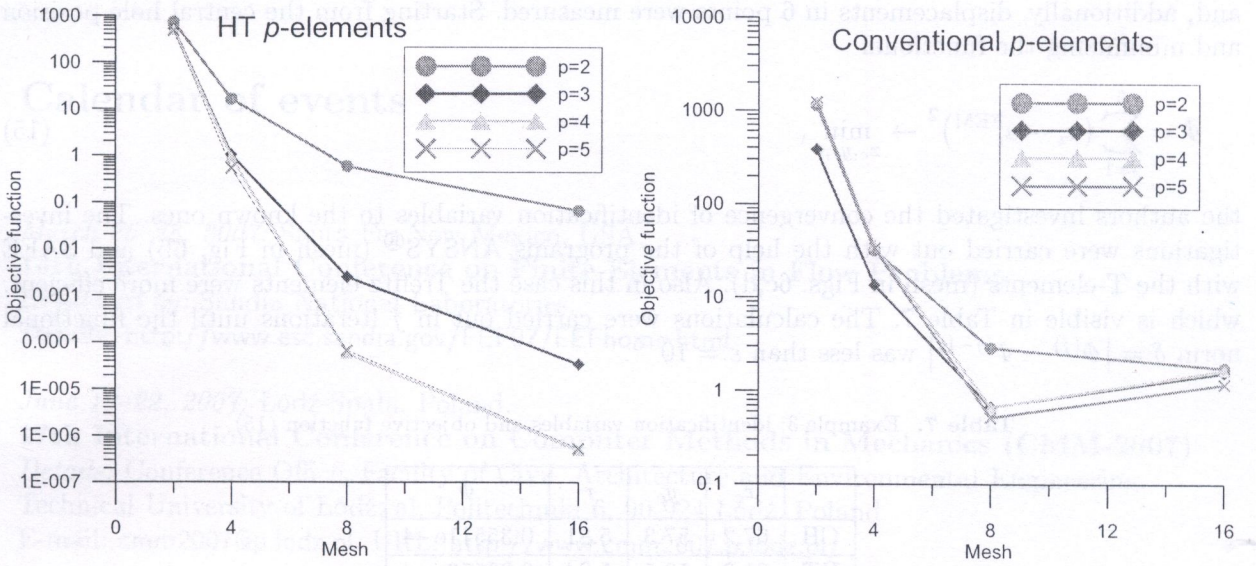

Fig. 5. Objective function (7) in example 2; $y_{cp} = 0.8$, $N = 21$

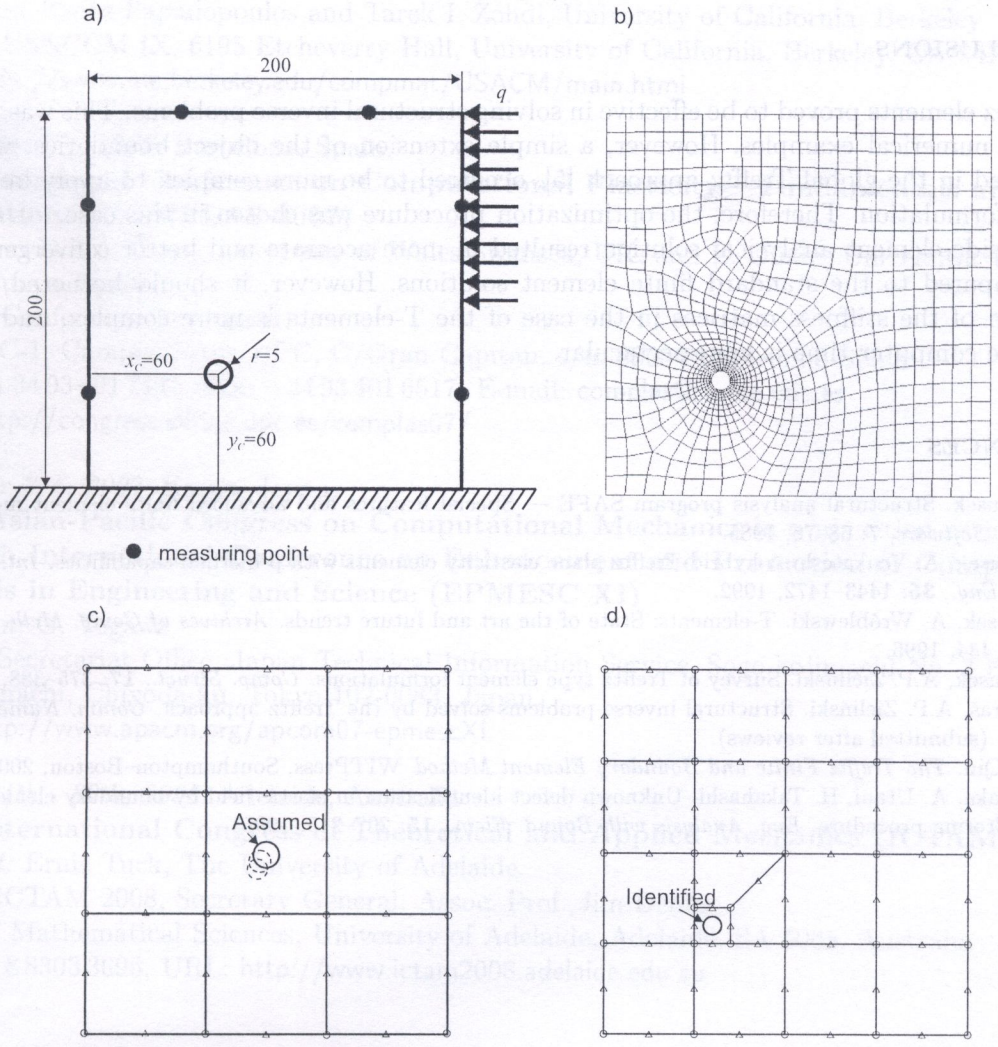

Fig. 6. Square plate for numerical simulation a) problem definition, b) final mesh from ANSYS® program, c) starting mesh of HT elements, d) final mesh of HT elements

and, additionally, displacements in 6 points were measured. Starting from the central hole position and minimizing the functional

$$\Phi = \sum_{i=1}^{6} \left(u_i - u_i^{\mathrm{FEM}}\right)^2 \to \min_{x_c, y_c, r} , \tag{15}$$

the authors investigated the convergence of identification variables to the known ones. The investigations were carried out with the help of the programs ANSYS® (mesh in Fig. 6b) and SAFE with the T-elements (mesh in Figs. 6c,d). Also in this case the Trefftz elements were more efficient, which is visible in Table 7. The calculations were carried out in j iterations until the functional norm $\delta = \left|\Phi^{(j)} - \Phi^{(j-1)}\right|$ was less than $\varepsilon = 10^{-5}$.

Table 7. Example 3: identification variables and objective function (15).

	x_c	y_c	r	Φ
CH	67.2	57.3	5.81	0.35511e−4
HT	61.3	58.5	5.24	0.32556e−4

4. Conclusions

The Trefftz elements proved to be effective in solving structural inverse problems. This was presented in several numerical examples. However, a simple extension of the object boundaries, which was investigated in the global Trefftz approach [5], occurred to be more complex to apply in the finite elements formulation. Therefore, the optimization procedure was chosen in this case.

The inside-element analytical solution resulted in more accurate and better convergent results when compared to the standard finite element solutions. However, it should be noted, that the calculation of the stiffness matrices in the case of the T-elements is more complex, and the final gain in the computer time is less spectacular.

References

[1] J. Jirousek. Structural analysis program SAFE — Special features and advanced finite element models. *Adv. Engng. Software*, **7**: 68–76, 1985.

[2] J. Jirousek, A. Venkatesh. A hybrid-Trefftz plane elasticity elements with p-method capabilities. *Int. J. Numer. Meth. Eng.*, **35**: 1443–1472, 1992.

[3] J.Jirousek, A. Wróblewski. T-elements: State of the art and future trends. *Archives of Comp. Meth. in Engng.*, **3**: 323–434, 1996.

[4] J. Jirousek, A.P. Zieliński. Survey of Trefftz type element formulations. *Comp. Struct.*, **17**: 375–388, 1997.

[5] M. Karaś, A.P. Zieliński. Structural inverse problems solved by the Trefftz approach. *Comm. Numer. Methods Engng.* (submitted after reviews).

[6] Q.-H, Qin. *The Trefftz Finite and Boundary Element Method.* WITPress, Southampton–Boston, 2000.

[7] N. Tosaka, A. Utani, H. Takahashi. Unknown defect identification in elastic field by boundary element method with filtering procedure. *Eng. Analysis with Bound. Elem.*, **15**: 207–215, 1995.